Slow Photon Generation on Silicon NanoPhotonic Crystal Waveguides and Applications

Yongqiang Jiang, Wei Jiang, Xiaonan Chen, Lanlan Gu, Brie Howley, Ray T. Chen*
Microelectronic Research Center, Department of Electrical and Computer Engineering,
The University of Texas at Austin, Austin, TX 78758, USA
* Email: chen@ece.utexas.edu
(Invited Paper)

ABSTRACT

Photonic crystal line defect waveguides show high group velocity dispersion and slow photon effect near transmission band edge. The group index of the fabricated silicon photonic crystal line defect waveguide is experimentally demonstrated as high as 45 at optical wavelength around 1558 nm. The group velocity dispersion of the fabricated silicon photonic crystal line defect waveguide is as high as 50 ps/nm·mm at wavelength around 1558 nm, which is more than 10^7 times the dispersion of the standard telecom fiber (D = 3 ps/nm·km). Due to the integration nature of photonic crystals, system-on-chip integration with multifunction including modulation, switching, delay manipulation, and detection can be easily achieved. Further results will be presented in the plenary session of the conference.

Keywords: Photonic crystal waveguide, group velocity dispersion (GVD), slow photon

I. INTRODUCTION

Photonic crystals (PhCs) have become a hot topic since 1990's. Nanophotonics including PhCs promises to have a revolutionary impact on the landscape of photonics technology. Photonic crystals are a new class of artificial optical materials with periodic dielectric structures, which result in unusual optical properties and promise to provide revolutionary solutions to the miniaturization of photonic devices. Photonic crystals with photonic band gaps (PBGs) are expected to be key platforms for future optical integrated circuits [1-11]. Due to its unique properties, the size of most optical components can be greatly reduced. In initial studies it seems that 3-D PhC structures with 3-D PBGs are essentially required to obtain these unique properties. However, recent studies show that 2-D PhC slab can also obtain very good performance [3]. PhC slabs are 2-D PhC structures located within the slab waveguide. In PhC slab, the light is confined by a combination of in-plane PBG confinement and vertical total-internal-reflection (TIR) confinement. One simple way to utilize the PBG effect is to introduce functional defects into PhCs, which is analogous to doping intentional defects in electronic crystals to introduce defect bands. Line defects can work as strongly confined waveguides. Due to all these unique properties and easy fabrication techniques, 2-D PhC slab line defect waveguides have been most extensively studied [4-7].

One of the most interesting and exciting properties is high group velocity dispersion and slow photon effect near transmission band edge. Notomi et al firstly demonstrated high group velocity dispersion and slow photon defect using silicon photonic crystal waveguide [4]. Several other groups also demonstrated this effect in both line defect and coupled cavity photonic crystal waveguide [5-8]. Insertion loss including propagation and coupling loss is also a very import factor for using these waveguide. Kuramochi et al demonstrated 0.5 dB/mm on silicon photonic crystal waveguide [9]. Barclay et al demonstrated 94% coupling efficiency by evanescent coupling between a silica optical fiber and a silicon PhC waveguide [10]. The total insertion loss is low enough for most practical application. In this letter, highly dispersive PhC waveguides are designed, fabricated and characterized.

II. DESIGN OF PHOTONIC CRYSTAL WAVEGUIDES

We use a W-1 line defect PhC waveguide design to achieve high group velocity dispersion or slow photon effect (high group index). The W-1 line defect photonic crystal waveguide can be easily generated by removing a single line defect from pure 2-D photonic crystal slab, as shown in Fig. 1. The slab is generated on a silicon-on-insulator wafer. The thickness of the silicon core layer is t = 220 nm. Top cladding is air and bottom cladding is buried oxide layer with thickness of 2 μm. The pitch size of the PhC is $a = 400\ nm$. The normalized air hole diameter is d/a = 0.55. The dispersion diagram of PhC waveguides can be calculated using the 3-D full vectorial plane-wave expansion (PWE) method, which is fast and accurate compared to other methods [20]. Since our PhC waveguide design is a 2-D PhC slab with line defects, we need to use a supercell having a size of N×M×L instead of a natural unit cell to implement the periodic boundary conditions. As shown in Fig. 1 a 7×1×5 supercell is used for simulation purposes. The simulated electrical and magnetic field intensities, $|E|^2$ and $|H|^2$, are also shown in Fig. 2. It shows that most of energy is guided around the defect inside the supercell. More simulation is done on the PhC waveguide. We can clearly see that the guided mode around the line defects, as shown in Fig. 2. We should notice here that normalized by the maximum intensity of the guided mode at the vertical

center of the silicon slab waveguide at Y = 0, the maximum intensity at Y = 54.8 nm is less than that at Y = -54.8 nm. The reason is that the guided mode decays faster in the top air layer than in the bottom buried oxide layer.

The dispersion parameter, ω(k), of PhC waveguide described above is also shown in Fig. 3(a). The bandgap is located between normalized frequencies $a/\lambda = 0.245 \sim 0.300$. The guided mode in the bandgap generated by introducing line defect is clearly shown here. The derived group index versus free-space optical wavelength is shown in Fig. 3(b). The large group index $n_g = 60$ is obtained around 1546 nm in this structure. The group index changes rapidly around the transmission band edge, which means high group velocity dispersion. The reason behind is due to the unusual flat of the guided mode around the transmission band edge in the dispersion diagram which leads to small group velocity thus high group index and large group velocity dispersion.

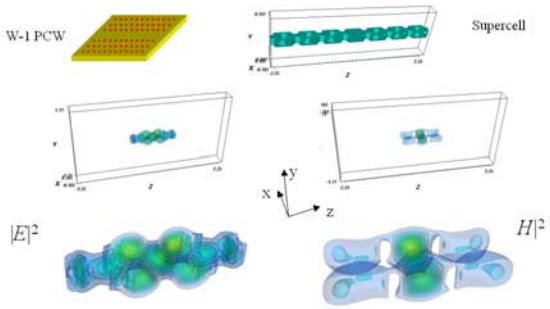

Fig. 1. Photonic crystal line defect waveguide schematic diagram, supercell used in simulation by 3-D full vectorial plane wave expansion method and electrical and magnetic filed intensity from the simulation.

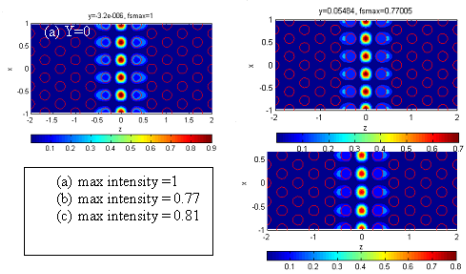

Fig. 2. Simulation of guided mode by 3-D full vectorial plane wave expansion method.

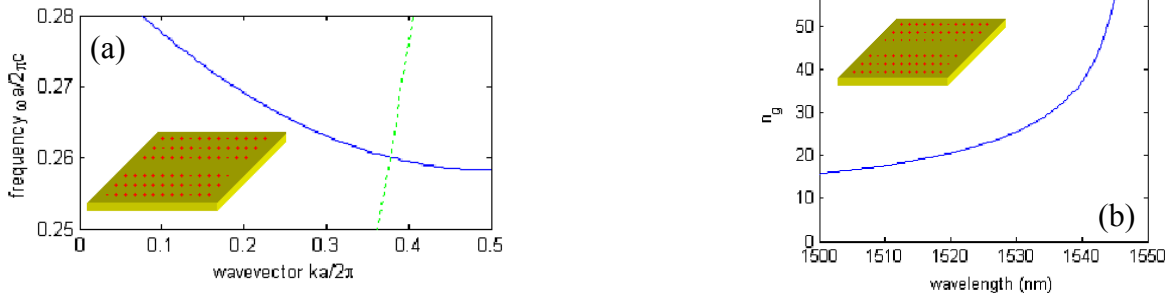

Fig. 3. (a) Dispersion diagram of a line defect photonic crystal slab waveguide by 3-D full vectorial plane wave expansion method. (b) Derived group index versus wavelength from dispersion diagram. High group index and large group velocity dispersion are clearly shown near transmission band edge at 1546 nm.

III. FABRICATION OF PHOTONIC CRYSTAL WAVEGUIDES

We fabricated photonic crystal waveguides (PCW) with silicon-on-insulator (SOI) based hexagonal periodic air-hole structures. We typically start with wet growing about 60 nm oxide at 850°C on top of a 6" SOI wafer. Then we cut it into about 1 cm × 1cm square pieces. First PhC structures are patterned with E-beam resist ZEP-520A by E-beam nano-lithography (JEOL JBX-6000FS/E, resolution: 20 nm). After resist developing, the patterns are transferred to 60 nm oxide mask layer by CHF_3 chemistry in RIE. Then the E-beam resist residue is removed by plasma ashing in O_2. Finally the patterns are transferred to silicon core layer with oxide as the mask layer by HBr and Cl_2 chemistry in RIE. On each chip, devices with lattice constant a = 400 nm, air hole diameter d = 220 nm, and slab thickness t = 220 nm are fabricated. Post-etching oxidation at 850° is implemented for about 1 minute. The post-etching oxidation forms an additional 6~7nm oxide layer, with a surface significantly smoother than the original silicon surface after the dry etching. The air holes of the silicon photonic crystals expand noticeably after the completing the entire fabrication sequence. E-beam resist exposure and development, dry-etching of the oxide hard mask and the SOI layer all incur certain amount of expansion of the holes. Dry-etching SOI layer appears to be the most critical step in hole size control. We have optimized the process parameters and have introduced a proper pre-offset of the hole size in e-beam pattern design so that the hole size can be controlled with an accuracy of 5%.

IV. CHARACTERIZATION OF PHOTONIC CRYSTAL WAVEGUIDES

1. Morphological examination

The nano-structures of silicon photonic crystal waveguide have been imaged by a FEI Strata DM235 SEM/FIB nano-characterization. A number of scanning electron microscopic (SEM) pictures are shown in Fig. 4(a), which demonstrates the high quality of the silicon nano-structures fabricated through our optimized processes. For reference, we show in Fig. 4(b) an early fabrication result where the post-etching oxidation was not employed. In addition, we have also used the focus ion beam (FIB) to polish the end-face of silicon rib waveguides. The resultant smooth end-face, as illustrated in Fig. 4(c) helps reduce the coupling loss between the silicon rib waveguide and the input fiber.

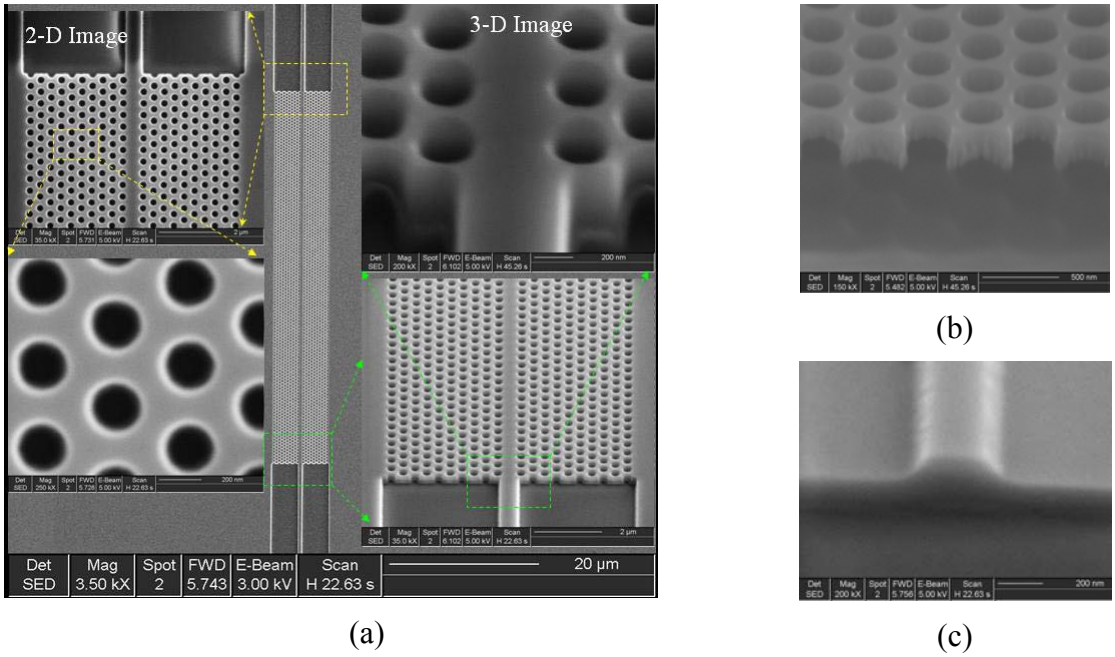

Fig. 4 SEM pictures of the nano-structures of silicon photonic crystal waveguides(PCW). (a) PCW fabricated *with post-etching oxidation*. An overview of a PCW is shown at the center. Details of this PCW are magnified successively, as indicated by colored frames and arrows. The waveguide is based on a triangular lattice with lattice constant a=400nm, hole diameter d=210nm, and SOI thickness t=215nm. (b) Photonic crystal sidewall profile when the post-etching oxidation is NOT performed. The surface roughness is evident. (c) The silicon rib waveguide end-face polished by focus ion beam (FIB); highly smooth surface facilitates coupling.

2. Measurement of optical transmission

We also accurately characterize the optical transmission and dispersion of photonic crystal waveguide modes. A simplistic approach places a PhC waveguide between two straight silicon rib waveguides. However, the stray light—light reaching the output through the air above the chip surface—in the forward direction is often strong enough to smear the signal transmitted via the rib-PCW-rib guided channel. To overcome this problem, we introduced a waveguide bend, which shifts the output fiber by at least 600µm and significantly suppresses the stray light collected by the output fiber. Two lensed fibers are manipulated by two automated 5-axis stages, which are controlled by a computer to precisely align the fibers with the rib waveguides. Fig. 5(a) shows a typical transmission spectrum of PhC waveguide with length 100a, which is normalized by the spectrum of a silicon rib waveguide (with the same bend and length). Below 1560nm, a guided mode is present in the gap. The bulge in the longer wavelength part of the spectrum is attributed to the lower band of the photonic crystal.

A 40µm-long PCW has typical loss of 6.5±2dB, while a 320µm-long PCW has typical loss of 8.3±3dB. From these, one can estimate the propagation loss is fairly low, about 6.4dB/mm. The coupling loss at each interface between a PCW and a Si rib waveguide is about 3.1dB. Note that the waveguides fabricated without post-etching oxidation [Fig. 4(b)] typically have propagation losses over 20dB/mm, which manifests the advantage of oxidation.

3. Group index and group velocity dispersion calculation

The group index $n_g=c/v_g$ is calculated *directly* from the varying Fabry-Perot oscillation period of transmission spectrum [4], which incurs high uncertainty and fluctuation of computed n_g values due to noise and finite wavelength

resolution of the spectrum. Similar problems occur in analyzing signals such digitized human voice, and the countermeasures are well established. Here we introduced a simple Windowed Fourier Transform (WFT) algorithm [12], which computes n_g from experimental transmission spectra with low fluctuation. Fig. 5(b) attests the high n_g as anticipated, which promises over 10 times reduction in delay line length. The group velocity dispersion is also calculated as 50 ps/nm·mm at 1558 nm. The dispersion is increased by 10^7 times compared to standard telecom LEAF fiber that has a dispersion parameter of 3 ps/nm·km.

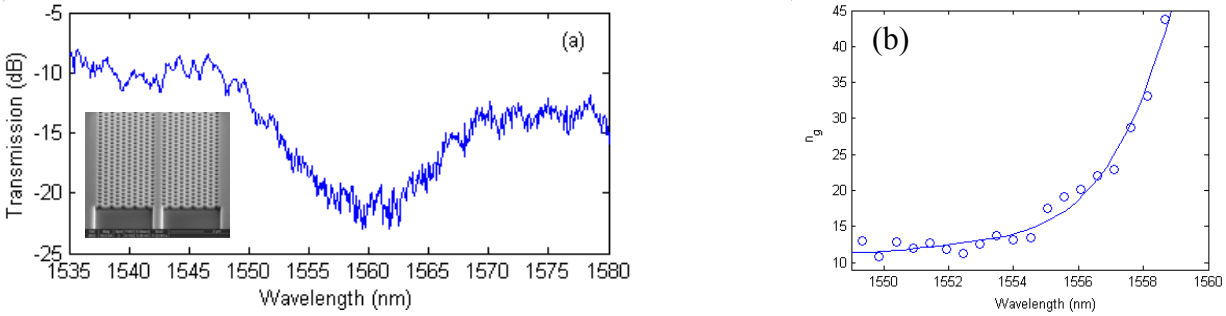

Fig. 5 (a) Transmission spectrum for a PCW with length 100a = 40μm, normalized by the spectrum of a Si rib waveguide. (b) Group index n_g a PCW, salient increases of n_g are evident. Good agreement with simulation results shown above.

V. CONCLUSION

Photonic crystal line defect waveguides show high group velocity dispersion and slow photon effect near transmission band edge. The group index of the fabricated silicon photonic crystal line defect waveguide is experimentally demonstrated as high as 45 at optical wavelength around 1558 nm. The group velocity dispersion of the fabricated silicon photonic crystal line defect waveguide is as high as 50 ps/nm·mm at wavelength around 1558 nm, which is more than 10^7 times the dispersion of the standard telecom fiber (D = 3 ps/nm·km).

ACKNOWLEDGMENT

This research is sponsored by AFOSR through Dr. Gernot Pomrenke's office. We thank the CNM at the UT Austin, Welch Foundation and SPRING for partial support of Dual Beam FIB/SEM usage. We also thank Dr. J. R. Cao of University of Southern California and Dr. B.R. Miao of University of Delaware at for fruitful discussions.

REFERENCES

[1] E. Yablonovitch, "Inhibited spontaneous emission in solid-state physics and electronics", Phys. Rev. Lett., vol. 58, pp. 2059-2062, 1987
[2] J.D. Joannopoulos, R.D. Meade, J.N. Winn, Photonic Crystals, Princeton University Press, 1995
[3] S.G. Johnson, S. Fan, P.R. Vileneuve, J.D. Joannopoulos, L.A. Kolodziejski, "Guided modes in photonic-crystal slabs," Phys. Rev. B, vol. 60, pp. 5751-5780, 1999
[4] M. Notomi, K. Yamada, A. Shinya, J. Takahashi, C. Takahashi, I. Yokohama, "Extremely large group velocity dispersion of line-defect waveguide in photonic crystal slabs", Phys. Rev. Lett., vol. 87, pp. 253902, 2001
[5] T. Baba, D. Mori, K. Inoshita, Y. Kuroki, "Light localizations in photonic crystal line defect waveguides", IEEE Journal of Selected Topics in Quantum Electronics, vol. 10, pp. 484 – 491, 2004
[6] T. Asano, K. Kiyota, D. Kumamoto, B.S. Song, S. Noda, "Time-domain measurement of picosecond light-pulse propagation in a two-dimensional photonic crystal-slab waveguide", App. Phys. Lett., vol. 84, 4690-4692, 2004
[7] D. Mori, T. Baba, "Dispersion-controlled optical group delay by chirped photonic crystal waveguides", App. Phys. Lett., vol. 85, pp. 1101-1103, 2004
[8] T.J. Karle, Y.J. Chai, C.N. Morgan, I.H. White, T.F. Krauss, "Observation of pulse compression in photonic crystal coupled cavity waveguide", Journal of lightwave technology, vol. 22, pp. 514-519, 2004
[9] E. Kuramochi, S. Hughes, T. Watanabe, L. Rumunno, A. Shinya, M. Notomi, "Low loss photonic crystal slab waveguides: fabrication, experiment, and theory", LEOS Annual Meeting, vol. 2, pp. 505 – 506, 2004
[10] P.E. Barclay, K. Srinivasan, M. Borselli, O. Painter, "Efficient input and output fiber coupling to a photonic crystal waveguide", Optics Letters, vol. 29, pp. 697-699, 2004
[11] S. G. Johnson and J. D. Joannopoulos, "Block-iterative frequency-domain methods for Maxwell's equations in a planewave basis," *Optics Express* **8**, pp.173-190, 2001
[12] A. V. Oppenheim, R. W. Schafer, Digital signal processing, Prentice-Hall, Upper Saddle River, 1975.